First excited $\frac{1}{2}^+$ state in ^{9}B

T. D. Baldwin,* W. N. Catford, D. Mahboub,† and C. N. Timis
Department of Physics, University of Surrey, Guildford, Surrey GU2 7XH, United Kingdom

N. I. Ashwood, N. M. Clarke, N. Curtis, and V. Ziman
School of Physics and Astronomy, University of Birmingham, Edgbaston, Birmingham B15 2TT, United Kingdom

T. A. D. Brown, S. P. Fox, B. R. Fulton, D. Groombridge, and D. L. Watson
Department of Physics, University of York, Heslington, York YO10 5DD, United Kingdom

V. F. E. Pucknell
CLRC Daresbury Laboratory, Daresbury, Warrington, Cheshire WA4 4AD, United Kingdom

D. C. Weisser
Department of Nuclear Physics, Research School Physical Sciences and Engineering, Bldg No. 57, The Australian National University, Canberra, ACT 0200, Australia

(Received 16 May 2012; published 24 September 2012)

Evidence has been found for a broad unbound state near 1 MeV excitation in ^{9}B that is a candidate for the long-disputed $\frac{1}{2}^+$ mirror of the unbound 1.68 MeV state in ^{9}Be. Reactions of ^{6}Li+^{6}Li were studied with a 60 MeV beam incident on a 240 μg/cm^2 ^{6}LiF target. The breakup fragments from the decay of the reaction products were detected in five Si-Si-CsI telescope detectors and the breakup particles were reconstructed using the technique of resonant particle spectroscopy. It is shown that contrary to a previous study, the $\frac{1}{2}^+$ is not populated in the reaction ^{6}Li(^{6}Li,t)^{9}B, but that it is populated via the ^{6}Li(^{6}Li,d)^{10}B reaction. The sequential decays of ^{10}B populated the channels ^{6}Li(g.s.)+α, ^{6}Li(2.186 MeV)+α, ^{8}Be+d, and $pn\alpha\alpha$, with the latter including (^{9}B+n or ^{9}Be+p) decay from ^{10}B. Decays through ^{9}B are identified and show the presence of the $\frac{1}{2}^+$ state as a broad asymmetric peak around 0.8–1.0 MeV with $\Gamma \approx 1.5$ MeV.

DOI: 10.1103/PhysRevC.86.034330 PACS number(s): 21.10.Sf, 23.50.+z, 27.20.+n, 25.70.Hi

I. INTRODUCTION

The concept of mirror nuclei is well established and mirror pairs such as ^{7}Li–^{7}Be, ^{13}C–^{13}N, ^{15}N–^{15}O, ^{17}O–^{17}F, and ^{19}F–^{19}Ne are known to have nearly identical energy level schemes [1]. The properties of the mass-9 system, in which the ^{9}B partner is particle unbound, even in the ground state, have been difficult to determine; the ground state is unbound to breakup into p+^{8}Be by 186 keV. There has been a large theoretical and experimental effort directed towards predicting and observing the low-lying states of ^{9}B, especially the first excited $\frac{1}{2}^+$ state. The unbound $\frac{1}{2}^+$ state at 1.68 MeV in the mirror ^{9}Be has been known for many years [2] and yet the existence and properties of the state in ^{9}B are not clear. The state is hard to define because it is difficult to excite and very broad. Furthermore, it exists amongst much more intensely populated peaks with large widths. Apart from the ground and 2.36 MeV states, all other $T = \frac{1}{2}$ states in this nucleus are broad with a width greater than 400 keV [3]. In addition, the nearby $\frac{5}{2}^-$ 2.36 MeV state is populated relatively intensely in the reactions that have so far been employed and there has often been a large background from multi-particle reactions [1]. It is clear that Lorentzian line shapes should be used to fit peaks, in preference to Breit-Wigner line shapes, due to the close proximity of the threshold and the high energy tails of the states [4,5], but this has not always been adopted in the analyses.

Conflicting theoretical predictions [3,6–11] exist for the energies of the mirror levels, using three different models. The argument between the two main theories centres around the Thomas-Ehrman effect [12–15]. The microscopic model of Descouvemont [9,10] and Arai [11] predicts the $\frac{1}{2}^+$ state in ^{9}B to be lower in energy than in ^{9}Be—in line with the usual Thomas-Ehrman shift. However, the R-matrix model of Barker [8] predicts the ^{9}B state to be higher in energy and therefore implies an inverted Thomas-Ehrman shift.

Previous experiments have reported observation of the first excited $\frac{1}{2}^+$ state in ^{9}B ranging from $E_x = 0.73 \pm 0.05$ MeV and width $\Gamma \approx 0.3$ MeV with a three state fit to ^{6}Li(^{6}Li,t) reaction data [16], to $E_x = 1.8 \pm 0.2$ MeV and width $\Gamma = 0.9 \pm 0.3$ MeV using the ^{10}B(^{3}He,α) reaction [17]. Numerous values between these have been reported [1,4,18–24]. The most recent results, using the (^{3}He,t) reaction [24], suggest tentative evidence for a broad state near 1.85 MeV but the study had a different focus and hence no real attempt was made to fit

*tam.baldwin@physics.org; Present address: Galson Sciences Ltd, 5 Grosvenor House, Melton Road, Oakham, Rutland, LE15 6AX, UK.
†Present address: Physics Department, University of Hail, PO Box 2440, Hail, KSA.

a realistic asymmetric lineshape to the $\frac{1}{2}^+$ resonance. In any case, the relevant region of excitation energy was dominated by the tails of other states in ^{9}B.

The current work was instigated by the results of two experimental papers: Tiede *et al.* [16] and Akimune *et al.* [25]. In 1995, Tiede [16] used the ^{6}Li(^{6}Li,t) reaction and carried out an R-matrix analysis with Lorentzian lineshapes that suggested the presence of $\frac{1}{2}^+$ and $\frac{1}{2}^-$ states, in addition to the four known excited states at 2.36, 2.79, 4.8, and 6.97 MeV. This paper appears to offer the best data so far with its reduced background, suppression of the interfering $\frac{5}{2}^-$ state and Lorentzian line shapes with R-matrix analysis, albeit with limited statistics. This work was also the first to include interference effects between the states, which could be a significant effect in these nuclei. The paper calculates a lower limit of 0.6 MeV for the $\frac{1}{2}^+$ excitation energy.

The later work by Akimune *et al.* [25] found no clear evidence for the presence of the low-lying $\frac{1}{2}^+$ state (although a peak was suggested at 1.8 MeV), but it did see a broad strongly excited state at 3.8 MeV. This paper called for the reanalysis of the Tiede [16] data to include this new state at 3.8 MeV because it may affect the contribution to the fitted spectrum from the $\frac{1}{2}^-$ state, and thus the $\frac{1}{2}^+$ state—this could then affect the previous results and provide definite information on low-lying ^{9}B structure.

Taking into account the limited statistics of the Tiede *et al.* [16] data, the points made by Akimune *et al.* [25] essentially called for a repeat of the original experiment with a more efficient setup, covering a larger angular area and supporting a much higher counting rate. The present work addresses that need.

II. EXPERIMENTAL PROCEDURE

A 60 MeV ^{6}Li^{3+} beam, provided by the Australian National University 14UD Tandem Pelletron Van de Graaff accelerator, was incident on a 95% ^{6}Li enriched 240 μg/cm^2 LiF target, backed with 20 μg/cm^2 ^{12}C [26]. The detection system consisted of five position sensitive ΔE-E detector telescopes (50 mm × 50 mm), composed of three stages at forward angles and two stages for the backward angle telescope. The four forward telescopes were used to detect the ^{9}B decay particles [^{9}B→ $p + (^8\text{Be}\rightarrow \alpha + \alpha)$]. These telescopes were composed of two Si detectors, the first 70 μm thick and segmented into four symmetric quadrants whilst the second was 500 μm thick and comprised 16 position-sensitive resistive strips orientated parallel to the reaction plane. The third stage of the forward telescopes was a 1 cm thick CsI detector. The backward angle telescope was used to detect the recoiling t from ^{6}Li(^{6}Li,t)^{9}B. This consisted of a Si quadrant (60 μm) and strip (500 μm) detector. The forward detectors were arranged symmetrically about the beam axis at 17° and 47°, 140.2 mm from the target (see Fig. 1). The rear detector was centered at 127.5° on the side opposite Telescope 1, at a distance of 55.2 mm.

This study of ^{9}B via the reaction (^{6}Li+^{6}Li)→ (^{9}B+t) → (^{8}Be+$p + t$) → ($\alpha + \alpha + p + t$) used resonant particle spectroscopy to reconstruct the reaction [27]. If the energy

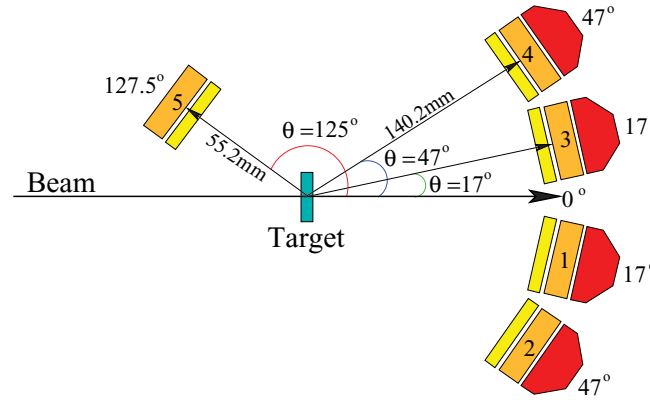

FIG. 1. (Color online) Plan view of the detector arrangement relative to the target. The four forward detectors were placed symmetrically about the beam axis at ±17° and ±47°, 140.2 mm from the target, whilst the rear detector was placed at 127.5° and 55.2 mm from the target.

and position of the two α particles from ^{8}Be decay are determined along with those of the p then the reaction can be fully reconstructed. The energy and momenta of the four particles can be used to calculate the relative velocities and energies between particles in the decay sequence, thus enabling reconstruction of the ^{9}B excitation energy spectrum. In fact, the t could also be detected directly in the rear telescope, thus producing significantly cleaner spectra.

The Si strip detectors were calibrated using elastic scattering of 40 MeV and 17.8 MeV ^{6}Li on a thin ^{197}Au target (5 μg/cm^2 on 10 μg/cm^2 ^{12}C), and 40 MeV ^{12}C on a 100 μg/cm^2 ^{12}C target. The ΔE Si quadrant detectors were measured using the scattering of 40 MeV ^{6}Li from gold to have average thicknesses of 58, 66, 67 and 69 μm. For Telescope 5 the ΔE thickness was measured to be 69 μm. The light output of CsI crystals is a nonlinear function of energy and significantly dependent on both A and Z, and hence a separate calibration was required for each nuclide. This was achieved using the energy deposited in the Si detectors.

The experiment trigger logic required two particles in the strip detector of Telescope 1 (normally due to two α particles from the ^{8}Be breakup) and software selection required a third event in any of the forward telescopes. The energy and position information for these events was used to calculate relative energies, momenta, breakup angles and reaction Q values. The selection of ^{8}Be ground state events was achieved by reconstructing the relative energies between pairs of particles in Telescope 1. A peak was observed corresponding to the ^{8}Be ground state at a relative energy of 90.11 ± 0.02 keV due to experimental resolution.

III. ANALYSIS

A. Reconstruction of ^{6}Li(^{6}Li,t)^{9}B→ $\alpha\alpha p$

The ^{6}Li(^{6}Li,t)^{9}B reaction produced ^{9}B that was forward focused in the laboratory frame, never exceeding 40°. The resultant breakup α particles were always stopped in the strip detector. The data were analysed separately, dependent upon

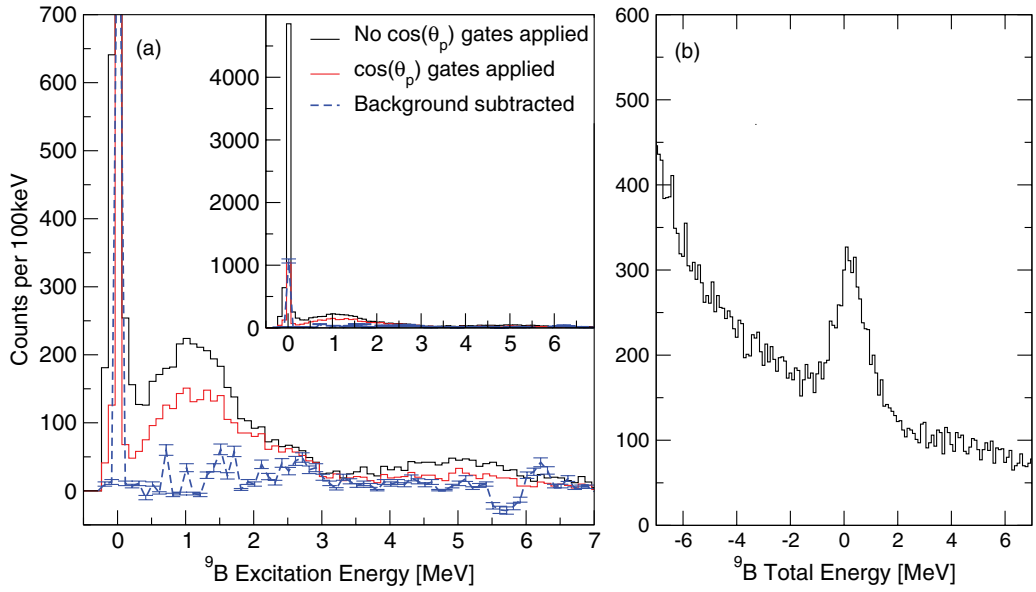

FIG. 2. (Color online) (a) Plot of reconstructed ^{9}B excitation energy for stopped $\alpha\alpha p$ events. In comparison to the upper solid (black) line, the middle (red) line corresponds to stopped p data with additional requirements on θ_p as described in the text; there is a 57% reduction in number of counts but efficiency becomes much less dependent on excitation energy. The lower dashed (blue) line additionally includes subtraction of the background beneath the relevant peak in the Q-value spectrum (b).

whether the protons punched through to the CsI or not. The protons start to punch through the strip detector and into the CsI stage when the ^{9}B excitation energy [$E_x(^9\mathrm{B})$] reaches $\sim$1.0 MeV. Once $E_x(^9\mathrm{B})$ exceeds $\sim$2.5 MeV, the majority of the detected ^{9}B events correspond to a punched through p.

In order to ensure that the ^{9}B efficiency was not strongly dependent on excitation energy, further cuts were introduced in the analysis, based on Monte Carlo simulations. The angle between the ^{9}B velocity vector and the p velocity in the ^{9}B reference frame (θ_p) was required to be in the range of $90^\circ < \theta_p \leqslant 120^\circ$ for the stopped proton data. Given that angular correlations exist in the breakup, restricting to a small angular range could in principle cut out a state of a particular spin; however, the state of interest has $L = 0$ and is therefore isotropic and this analysis was not used to look at other states. Figure 2(a) shows the effects of imposing the limited proton angular range on the experimental $E_x(^9\mathrm{B})$ spectra. The reconstructed total energy (or Q value) spectrum shows a peak corresponding to ^{6}Li(^{6}Li,t)^{9}B [see Fig. 2(b)], and the region of the peak was used to select the reaction. Using gates above and below the Q-value peak in Fig. 2(b), the background under the peak was subtracted. The background subtracted spectrum is also included in Fig. 2(a) and shows clearly that the majority of the peak near 1.0 MeV in ^{9}B arises from some mechanism other than the ^{6}Li(^{6}Li,t)^{9}B reaction.

This conclusion was confirmed by analyzing ^{6}Li(^{6}Li,t)^{9}B data in which the coincident t was detected in Telescope 5. The measured angle of the t was required to match the angle calculated from the reconstructed ^{9}B angle. This selected approximately one third of the counts in the $\alpha\alpha p$ data set with very little contamination. The ground state and $\frac{5}{2}^+$ 2.8 MeV excited state peaks were clearly observed but there was no evidence at all for a peak near 1.0 MeV.

B. Reconstruction of ^{6}Li(^{6}Li,d)^{10}B$\rightarrow$ $pn\alpha\alpha$

From an investigation of other possible reaction channels the most populous reaction was found to be ^{6}Li(^{6}Li,d)^{10}B—the d ejectile kinematic curves from this reaction were present in plots of energy against angle for Telescope 5 with the most intense d curve corresponding to $E_x(^{10}\mathrm{B}) = 4.77$ MeV. The sequential decays ^{10}B that were observed in this experiment were ^{6}Li(^{6}Li,d)α^6Li(gs), ^{6}Li(^{6}Li,d)α^6Li*, ^{6}Li(^{6}Li,d)d^8Be, and ^{6}Li(^{6}Li,d)$pn\alpha\alpha$.

For (^{6}Li,d) producing ^{10}B, the final decay products ($pn\alpha\alpha$) can be obtained via $^{10}\mathrm{B} \rightarrow {}^9\mathrm{B}+n$ (threshold of 8.44 MeV) or via $^{10}\mathrm{B} \rightarrow {}^9\mathrm{Be}^*+p$ (threshold of 6.59 MeV). Note that ^{10}B decay to the ^{9}Be ground state does not result in $pn\alpha\alpha$ decay particles because the ^{9}Be ground state is stable. The ^{9}Be(g.s.)+p channel was not observed due to the vanishingly small probability for both the p and ^{9}Be to enter Telescope 1 and satisfy the trigger requirements.

As the final decay particles included an undetected neutron, all of the remaining reaction particles ($dp\alpha\alpha$) had to be detected and this lowered the statistics greatly. Events were selected by requiring two particles in Telescope 1 to give a count in the ^{8}Be ground state relative energy peak. A third forward particle was required and was identified to be a stopped or punched through p depending on whether it reached the CsI detector. A particle was also required in Telescope 5 and taken to be the associated d. Any missing momentum was assumed to be due to an undetected n. The missing n energy showed the appropriate correlation with the missing momentum.

Events satisfying this correlation were used to reconstruct the ^{10}B excitation energy. No clear peaks were observed in the resulting ^{10}B excitation spectrum. Correlations between $\alpha\alpha p$ and $\alpha\alpha n$ were sought by comparing ^{8}Be+p and ^{8}Be+n relative energies in a two-dimensional plot. The projected ^{9}B

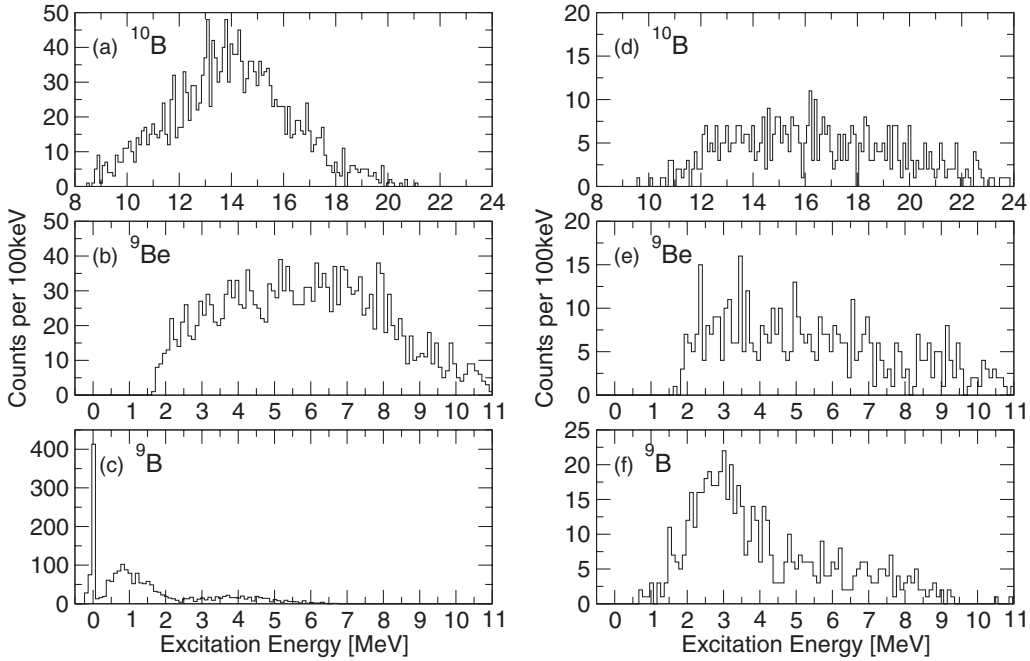

FIG. 3. Data from ^{6}Li(^{6}Li,d)^{10}B$\rightarrow$ $pn\alpha\alpha$: ^{10}B, ^{9}Be, and ^{9}B obtained for data from the reaction ^{6}Li(^{6}Li,d)^{10}B$\rightarrow$ $pn\alpha\alpha$ for the stopped proton data [spectra (a), (b), and (c)] and the punched through proton data [spectra (d), (e), and (f)].

and ^{9}Be excitation energy spectra for these data show no correlations denoting ^{9}Be states. The bound ^{9}Be ground state would obviously not be observed in this reconstruction but there is no evidence for any other states either, such as the first excited state at 1.68 MeV. Similar results were obtained for the punched through p data, with clear support for the ^{9}B state at 2.8 MeV excitation and no evidence for any ^{9}Be states.

As in the ^{6}Li(^{6}Li,t) analysis, the proton angle relative to the ^{10}B vector was limited to be between 90° and 120° for the stopped proton data in order to achieve a detection efficiency with only a weak dependence on excitation energy. The reconstructions for ^{10}B and the excitation energy spectra for ^{9}B and ^{9}Be with all gates applied are shown in Fig. 3.

No evidence for the decay ^{10}B$\rightarrow$ p+^{9}Be is found in Fig. 3. Decay of ^{10}B to ^{9}Be has been observed before, by Leask *et al.* [29] using the reaction ^{7}Li(^{12}C,^{10}B*)^{9}Be with a beam energy of 76 MeV, and by Curtis *et al.* [30] using Li_2O(^{7}Li,^{10,11,12}B*) at 58 MeV. However, both these experiments were designed to detect only the ground state ^{9}Be bound particle, not its excited breakup particles, whereas the opposite is true here. Both papers also noted that this was a very weak decay channel from ^{10}B and that α decay channels were dominant.

This experiment populated ^{10}B up to approximately 19 MeV which is well above the combined ^{9}Be*(1.68 MeV) + p threshold and Coulomb barrier of 8.8 MeV (6.58 and 2.22 MeV, respectively). Note that the 1.68 MeV state in ^{9}Be is the lowest state that can decay into $\alpha + \alpha + n$. All known states in ^{10}B above the barrier, apart from the 11.52 MeV state, are known to p decay [28]. However, clear peaks may be absent in the reconstructed ^{9}Be excitation energy spectra compared with ^{9}B spectra, because ^{9}B is reconstructed from three detected particles ($\alpha\alpha p$), but ^{9}Be is reconstructed from two detected particles and suffers from the low resolution obtained for the reconstructed neutron.

In summary, the ^{6}Li(^{6}Li,d)n^{9}B data for the stopped proton [Fig. 3(c)] show an additional clear peak just below 1 MeV that is not populated via ^{6}Li(^{6}Li,t)^{9}B, but is populated via the sequential decay of ^{10}B from ^{6}Li(^{6}Li,d)^{10}B*. The peak is a good candidate for the first excited ^{9}B $\frac{1}{2}^{+}$ state and this analysis therefore supports population of the $\frac{1}{2}^{+}$ state in ^{6}Li+^{6}Li. The peak shapes at 1.0 MeV in both Figs. 2 and 3 are comparable and the ratios of the ground state and 1.0 MeV peak areas are similar.

C. Monte Carlo simulation of detection efficiency

The various ^{6}Li+^{6}Li reactions were simulated and the efficiencies for the multiparticle breakup channels calculated using the Monte Carlo program RESOLUTION8 [31]. Experimental resolutions for reconstructed reactions were also predicted. The same gates and limits applied to the real experimental data were applied to the Monte Carlo simulated data, including the individual detector thresholds and the gate on θ_p, the angle between ^{9}B and the emitted proton. Events that produce ^{9}B via the ^{6}Li(^{6}Li,d)^{10}B reaction proceed through a range of ^{10}B excitation energies. The midpoint of the experimentally populated ^{10}B was observed to be approximately 15 MeV and this energy was adopted in the simulation.

The simulations give efficiency curves that are understandable. The ^{9}B ground state peak is formed from events where both the proton and the ^{8}Be are detected in Telescope 1. The angle between the two particles then increases with

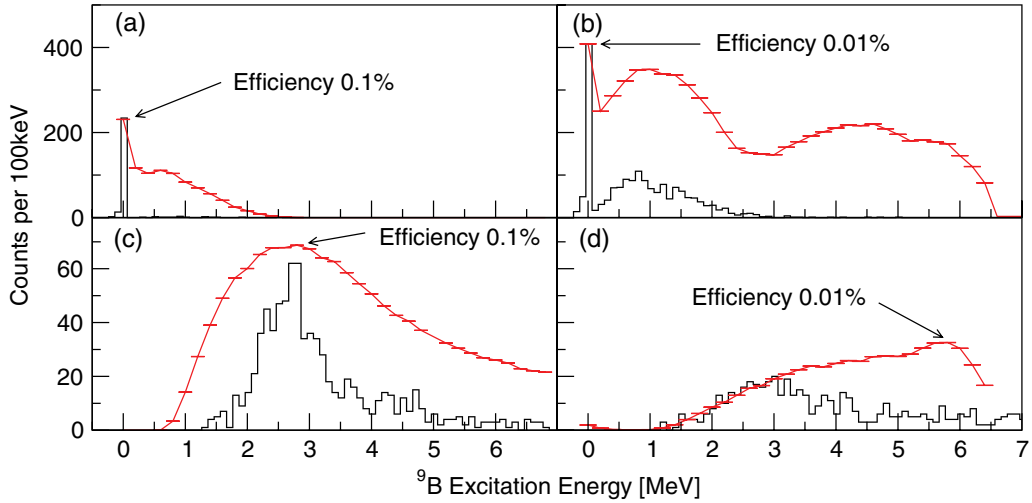

FIG. 4. (Color online) Final ^{9}B experimental spectra (black/lower) overlaid with the calculated efficiencies (red/upper) as described in the text: (a) and (c) data from the ^{6}Li(^{6}Li,t)^{9}B reaction; (b) and (d) data from the ^{6}Li(^{6}Li,d)^{10}B reaction. The protons either stopped in the strip detector [(a) and (b)] or punched through to the CsI [(c) and (d)].

the increasing relative energy such that the proton starts to miss Telescope 1. The detection efficiency falls when the p has sufficient relative energy to sometimes miss Telescope 1 but not reach the neighboring Telescopes 2 or 3. The efficiency rises between 0.5 MeV and 2.5 MeV when these telescopes are in range and then falls again by 3 MeV when the proton increases its angle such that it needs to reach the outermost detector, Telescope 4. Around 2.5 MeV the increased proton relative energy means the proton may punch through the strip detector into the CsI. The simulations led to the θ_p limits being changed to between 75.5° and 98.6° for the stopped proton reconstructions in order to make the efficiency profiles as smooth and slowly varying as possible. Further, for the punched through data, it was required that the proton must be detected in a different forward telescope than the ^{8}Be.

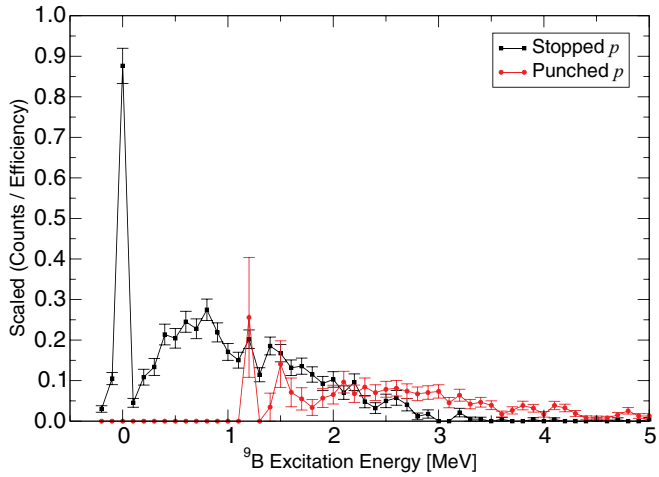

FIG. 5. (Color online) Excitation energy spectrum for ^{9}B from the ^{6}Li(^{6}Li,d)^{10}B reaction, showing the stopped and punched through p data after correction for detection efficiency.

Figure 4 shows the final experimental ^{9}B spectra, taking into account the revised gating prompted by the simulations. The figure includes data for punched through and stopped protons, for the ^{6}Li(^{6}Li,t)^{9}B and ^{6}Li(^{6}Li,d)^{10}B reactions, where a coincident particle was detected in Telescope 5. Note that the efficiency for ^{6}Li(^{6}Li,t) is an order of magnitude higher than for ^{6}Li(^{6}Li,d), reflecting the fact that the experiment was designed to study the ^{6}Li(^{6}Li,t) reaction because of the initial motivation to extend the work of Tiede *et al.* [16]. The ^{6}Li(^{6}Li,d)^{10}B reaction data of Fig. 4(b) show a broad peak supporting the existence of the $\frac{1}{2}^+$ state in ^{9}B. The punched through proton efficiency is almost zero in the $\frac{1}{2}^+$ region, but the data for ^{6}Li(^{6}Li,t)^{9}B clearly indicate detection of the 2.8 MeV excited state.

Figure 5 compares the stopped and punched through proton data for the (^{6}Li,d) reaction, after each has been corrected for the dependence of efficiency on ^{9}B excitation energy. This shows that, despite having substantially different efficiency corrections, the two data sets are in very reasonable agreement through the tail of the 1 MeV peak. No clear evidence exists for the population of any higher-lying levels above the 1 MeV peak. The punched through proton data have poorer statistical accuracy and are not considered further.

A final check on consistency in the data was achieved by selecting different angular ranges for the deuteron from (^{6}Li,d) in Telescope 5. Spectra for ^{9}B from stopped p data were obtained for three equal ranges: (a) 103.1°–119.4°, (b) 119.4°–135.7°, and (c) 135.7°–151.9°. The observed peak shape is consistent across all the spectra.

D. Barrier transmission effects for ^{10}B→^{9}B+n evaporation

The reaction ^{6}Li(^{6}Li,d)^{10}B in this experiment populates a range of ^{10}B excitation energies, with limits determined by experimental efficiency and matching conditions. The excited ^{10}B will decay with differing probabilities to different breakup

TABLE I. Threshold energies and Coulomb barrier heights (light ion and heavy ion) for ^{10}B decay channels. All energies are in MeV.

Channel	Threshold (a)	LI barrier[a] (b)	HI barrier[b]	Sum (a + b)
^{9}Be+p	6.58	2.22	1.50	8.80
^{9}B+n	8.44	–	–	8.44
^{8}Be+d	6.03	2.30	1.41	8.33
^{6}Li+α	4.46	3.80	2.03	8.26

[a]Using radius of core $1.25 \times A_1^{1/3}$.
[b]Using radius $1.25 \times (A_1^{1/3} + A_2^{1/3})$.

channels, as discussed with reference to previous experiments in Sec. III B. The analyses for the p, d, and α channels observed in this work are presented elsewhere [26]. The decay energies for the possible particle emission channels are shown in Table I, together with the height of the Coulomb barrier (using both the light ion and heavy ion conventions for radius). Comparing with the excitation energy at which ^{10}B is populated for the events in Fig. 3(a), it is evident that the different decay channels will compete according to structural and angular momentum effects. Considering the neutron channel, the branching to different states in ^{9}B will be influenced by the ability of the n to tunnel through the centrifugal barrier out of the ^{10}B nucleus. To the extent that the (^{6}Li,d) reaction involves α-particle transfer to the $0p$ and $1s0d$ shells, the evaporated n will be from an orbital with $L = 0$, 1, or 2. For each of these L values, the transmission is calculated (Section 5.4 of [26]) to be a weakly varying function of the final ^{9}B excitation energy, over the range 0–2 MeV (for a ^{10}B excitation energy of 15 MeV). To apply any correction for this effect requires too many assumptions to be useful, but the conclusion is that any effect on the lineshape of the peak near 1 MeV is small. The final spectrum for this excitation region, with efficiency correction, is extracted from Fig. 5 and reproduced in Fig. 6.

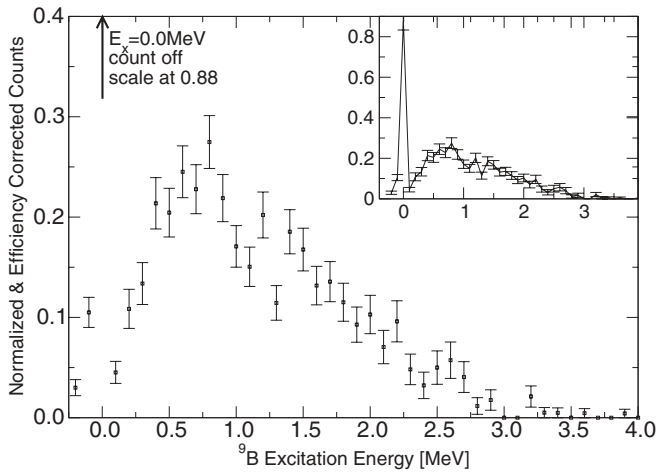

FIG. 6. Normalized and efficiency corrected ^{9}B excitation energy spectrum from the stopped p data. The vertical axis shows relative counts per 100 keV.

IV. CONCLUSION

The kinematic reconstruction of ^{9}B events from $\alpha\alpha p$ coincidences with deuterons in the ^{6}Li(^{6}Li,d)$pn\alpha\alpha$ reaction provides clear evidence for the ^{9}B ground state, the known excited $\frac{5}{2}^+$ state and an additional clear peak just below 1 MeV that is a good candidate for the first excited $\frac{1}{2}^+$ state. The 1 MeV peak is clear in the raw data of Fig. 4. Monte Carlo simulations assist the interpretation. The simulated efficiency for the ^{6}Li(^{6}Li,t)^{9}B reaction shows that although no counts were observed in the 1.0 MeV region, there is still reasonable detection efficiency. This confirms that the ^{9}B $\frac{1}{2}^+$ state, which is absent from the experimental spectra, is not populated in (^{6}Li,t). The ^{6}Li(^{6}Li,d)n^{9}B efficiency was found through simulations to be a factor of 10 smaller than that for the ^{6}Li(^{6}Li,t)^{9}B reaction for which the experiment was originally designed. The efficiency corrected spectra confirm the presence of a ^{9}B $\frac{1}{2}^+$ candidate peak near 1 MeV excitation.

The different selectivity of the two reactions for populating the $\frac{1}{2}^+$ candidate can probably be explained by the two-step nature of the (^{6}Li,d) pathway, which proceeds via transfer to a highly excited state in ^{10}B, followed by evaporation. Whereas the transferred ^{3}He in the (^{7}Li,t) reaction would need to show a strong overlap with a $(0p)^2 1s_{1/2}$ configuration, the transferred α particle in (^{6}Li,d) need only produce an overlap with some component of the wave function of the excited ^{10}B. In the region of excitation energy near 11–18 MeV, states in ^{10}B are likely to be a mixture of configurations and another component might easily have a large overlap with the ^{9}B+n decay channel.

The spectra of Tiede *et al.* [16] are similar to those obtained in this experiment for the ^{6}Li(^{6}Li,t)^{9}B reconstruction when only forward-going particles are detected. Note that the Tiede data are unlikely to be entirely from the (^{6}Li,t) reaction as claimed and in fact the counts in the 1 MeV region arise mainly from the ^{6}Li(^{6}Li,d)^{10}B(n)^{9}B reaction, as demonstrated in the present work. This means that the efficiency corrections carried out on the data in that work were not appropriate.

The peak observed near 1 MeV (see Fig. 6) is very broad and displays an asymmetric lineshape as expected, tailing towards high energy. It is concluded that the $\frac{1}{2}^+$ resonance candidate peak lies in the range of 0.8 MeV to 1.2 MeV, with a peak just below 1.0 MeV and with a width slightly broader than 1 MeV. The peak has counts down to low energies, which is in agreement with the findings of Kadija *et al.* [4]. These properties are unlikely to be changed significantly by reaction mechanism effects such as the transmission of the evaporated neutron in the sequential ^{10}B$\rightarrow^{9}$B+n decay. Hence, the present result implies a normal Thomas-Ehrman shift.

ACKNOWLEDGMENTS

The authors wish to thank P. Barber of Florida State University for the provision of the LiF targets, and A. J. Bartlett, D. K. Baxter, N. K. Timofeyuk, and S. J. Williams for useful discussions.

[1] J. J. Kroepfl and C. P. Browne, Nucl. Phys. A **108**, 289 (1968).
[2] T. Lauritsen and F. Ajzenberg-Selove, Nucl. Phys. **78**, 1 (1966).
[3] R. Sherr and G. Bertsch, Phys. Rev. C **32**, 1809 (1985).
[4] K. Kadija, G. Paić, B. Antolković, A. Djaloeis, and J. Bojowald, Phys. Rev. C **36**, 1269 (1987).
[5] W. N. Catford, L. K. Fifield, E. L. Reber, K. W. Kemper, and J. D. Brown, Nucl. Phys. A **550**, 517 (1992).
[6] R. Sherr and H. T. Fortune, Phys. Rev. C **70**, 054312 (2004).
[7] H. T. Fortune and R. Sherr, Phys. Rev. C **73**, 064302 (2006).
[8] F. C. Barker, Aust. J. Phys. **40**, 307 (1987).
[9] P. Descouvemont, Phys. Rev. C **39**, 1557 (1989).
[10] P. Descouvemont, Eur. Phys. J. A **12**, 413 (2001).
[11] K. Arai, P. Descouvemont, D. Baye, and W. Catford, Phys. Rev. C **68**, 014310 (2003).
[12] R. G. Thomas, Phys. Rev. **88**, 1109 (1952).
[13] J. B. Ehrman, Phys. Rev. **81**, 412 (1951).
[14] S. Shlomo, Rep. Prog. Phys. **41**, 957 (1978).
[15] B. K. Agrawal, T. Sil, S. K. Samaddar, J. N. De, and S. Shlomo, Phys. Rev. C **64**, 024305 (2001).
[16] M. A. Tiede, K. W. Kemper, N. R. Fletcher, D. Robson, D. D. Caussyn, S. J. Bennett, J. D. Brown, W. N. Catford, C. D. Jones, D. L. Watson, and W. D. M. Rae, Phys. Rev. C **52**, 1315 (1995).
[17] N. Arena, Seb. Cavallaro, G. Fazio, G. Giardina, A. Italiano, and F. Mezzanares, Europhys. Lett. **5**, 517 (1988).
[18] J. B. Marion, C. F. Cook, and T. W. Bonner, Phys. Rev. **94**, 802 (1954).
[19] J. B. Marion, T. W. Bonner, and C. F. Cook, Phys. Rev. **100**, 91 (1955).
[20] R. J. Slobodrian, H. Bichsel, J. S. C. McKee, and W. F. Tivol, Phys. Rev. Lett. **19**, 595 (1967).
[21] G. D. Symons and P. B. Treacy, Phys. Lett. **2**, 175 (1962).
[22] F. C. Barker and P. B. Treacy, Nucl. Phys. **38**, 33 (1962).
[23] M. Burlein, H. T. Fortune, P. H. Kutt, R. Gilman, R. Sherr, and J. D. Brown, Phys. Rev. C **38**, 2078 (1988).
[24] C. Scholl, Y. Fujita, T. Adachi, P. von Brentano, H. Fujita, M. Górska, H. Hashimoto, K. Hatanaka, H. Matsubara, K. Nakanishi, T. Ohta, Y. Sakemi, Y. Shimbara, Y. Shimizu, Y. Tameshige, A. Tamii, M. Yosoi, and R. G. T. Zegers, Phys. Rev. C **84**, 014308 (2011).
[25] H. Akimune, M. Fujimura, M. Fujiwara, K. Hara, T. Ishikawa, T. Kawabata, H. Utsunomiya, T. Yamagata, K. Yamasaki, and M. Yosoi, Phys. Rev. C **64**, 041305(R) (2001).
[26] T. D. Baldwin, Ph.D. thesis, University of Surrey, 2006.
[27] W. D. M. Rae, A. J. Cole, B. G. Harvey, and R. G. Stokstad, Phys. Rev. C **30**, 158 (1984).
[28] D. Tilley, J. Kelley, J. Godwin, D. Millener, J. Purcell, C. Sheu, and H. Weller, Nucl. Phys. A **745**, 155 (2004).
[29] P. J. Leask, M. Freer, N. M. Clarke, B. R. Fulton, C. D. Freeman, S. M. Singer, W. N. Catford, N. Curtis, K. L. Jones, R. L. Cowin, D. L. Watson, R. P. Ward, N. A. Orr, and V. F. E. Pucknell, Phys. Rev. C **63**, 034307 (2001).
[30] N. Curtis, N. I. Ashwood, W. N. Catford, N. M. Clarke, M. Freer, D. Mahboub, C. J. Metelko, S. D. Pain, N. Soić, and D. C. Weisser, Phys. Rev. C **72**, 044320 (2005).
[31] N. Curtis, computer code RESOLUTION8, February 2006 version, unpublished.